

Tools of Nanotechnology: Electrospray

Oleg.V. Salata*

Sir William Dunn School of Pathology, University of Oxford, South Parks Road, Oxford, OX1 3RE, UK

Abstract: Liquids can readily interact with electric fields. Field-induced or injected charges in liquids interact with an external electric field causing liquids to move, break into drops or spray into jets or strings of fine droplets. One important case of liquid in the capillary deserves special mentioning as it serves as a basis of many and varied technological applications. An electric field acts on a liquid meniscus, counteracted by surface tension. In a strong enough field a cone is formed that emits a jet of liquid from its tip. This effect is used, for example, to coat car bodies by a thin uniform layer of paint. At the other end of the scale nano-electrospray has revolutionised mass-spectroscopy of bio-molecules. The ability of electrospray to repeatedly generate very small and uniform volumes of liquid makes it into one of the important tools of nanotechnology. Electrospray has been used to deposit ultra-thin films of inorganic, organic and biological materials, to generate nanoparticles and quantum dots, to sort them according to their sizes, and to help with dispersion and delivery of nanomaterials. This mini-review introduces basics of electrospray technology and summarises the diverse applications of electrospray in nano-sciences.

Keywords: Electrospray, nanoparticles, quantum dots, size separation, nanobiomaterials.

1. INTRODUCTION

Liquids can readily interact with electric fields. The interaction of field induced or injected charges in liquids with external electric field causes liquids to move, break into drops or spray into jets or strings of fine droplets. Lord Rayleigh was first to describe instabilities of a charged liquid drop back in 1882 [1].

One important case of liquid in the capillary deserves special mention as it serves as a basis of many and varied technological applications. An electric field acts on a liquid meniscus, counteracted by a surface tension. In a strong enough field a cone is formed that emits a jet of liquid from its tip. This jet breaks into plume due to the Rayleigh instability of the charged liquid. The first scientific observation of this phenomenon was reported by the physicist John Zeleny in 1914 [2]. The physics of interaction of a liquid in capillaries with electric fields was established forty years ago by Taylor [3].

Practical use of that interaction has appeared at an early stage [4,5]. The simplicity of electrospray generation is nicely illustrated in Fig. (1). More diverse applications followed. For example, car bodies are coated by a thin uniform layer of paint, thanks to use of electrospray gun [6]. Also, crop-dusting with insecticides relies on the same idea. At the other end of the scale application of nano-electrospray has revolutionised mass-spectroscopy of bio-molecules [7,8]. The benefits of electrospray include high material deposition efficiency as the droplets are moved and directed by the electrostatic force, simplicity of experimental set up and great flexibility in the choice of starting materials, which

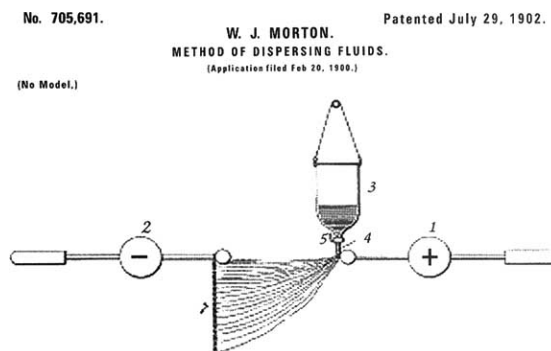


Fig. (1). The early illustration of electrospray principle

results in a broad range of compositions and morphologies. The ability of electrospray to repeatedly generate very small and uniform volumes of liquid [9] also makes it into one of the important tools of nanotechnology.

Electrospray has been used to generate nanoparticles and quantum dots [10-14], to deposit ultra-thin films of inorganic, organic and biological materials [15-18], to sort nanoparticles according to their sizes [19], and to help with dispersion and delivery of nanomaterials [20-22]. It is also an essential process in electro-spinning of nanofibres [23] and nano-encapsulation [24]. This mini-review introduces basics of the electrospray technology and summarises the diverse applications of electrospray in nano-sciences. As the word "mini" implies we are unable to include every single publication that involves electrospray. Of course, the electrospray itself is just a subset of more general aerosol or gas phase techniques and interested readers can find more information on that elsewhere, for example, in [25,26].

2. ELECTROSPRAY BACKGROUND

It was Lord Rayleigh [1] who, in 1882, wrote that an excessive charge q on the droplets of liquid would lead to

*Address correspondence to this author at the Sir William Dunn School of Pathology, University of Oxford, South Parks Road, Oxford, OX1 3RE, UK; Tel: +44-(0) 1865-285759; Fax: +44-(0) 1865-275515; E-mail: oleg.salata@path.ox.ac.uk

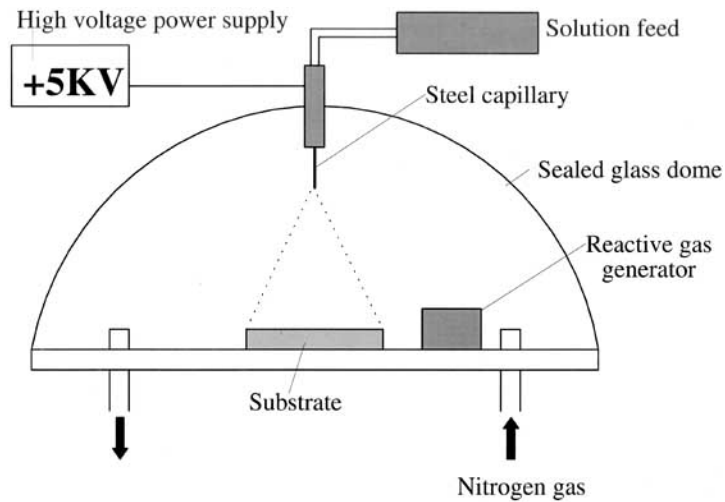


Fig. (2). Typical layout of an electro spray apparatus.

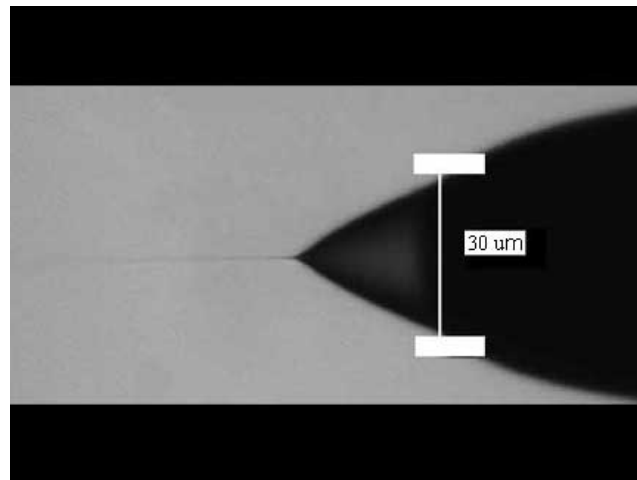


Fig. (3). Taylor cone-jet mode obtained with 30 μm capillary (photo courtesy of Dr. Peter Rockett, Department of Engineering Science, University of Oxford).

their disintegration as soon as the repulsive force between the charges on the droplet surface exceeds surface tension. The chances of droplet disintegrating can be described by “fissility” X , which is a ratio of electrostatic repulsion force to the surface force:

$$X = \frac{q^2}{64 \pi^2 \epsilon_0 R^3} \quad (1)$$

Rayleigh has demonstrated that for $X < 1$ the spherical form of the charged droplet is preserved. However, as X is getting closer to 1, a shape instability caused by increased charge repulsion results in the elongation of the drop, turning it into an ellipsoid. Eventually, continuing elongation results in the droplet partitioning into two smaller identical droplets of equal charge. The case of $X \gg 1$ was described by Rayleigh only in words, stating that, “the liquid is thrown out in fine jets, whose fineness however has a limit”. It was observed recently using microphotography that fine jets are produced even at $X = 1$ [27]; the authors have suggested that an old theory needs revision.

In a typical electro spray set up (Fig. (2)) an accumulation of charges on the surface of the liquid makes the surface unstable and leads to the formation of the Taylor cone (Fig. (3)), usually with an angle close to the predicted static half angle of 49.3° [10].

However, some deviations and alternative stable angles are possible for high viscosity liquids, e.g. polymer solutions [28]. The onset voltage required to start jet production is proportional to the square root of the surface tension multiplied by the radius of the capillary orifice. The higher the onset voltage the greater are the chances of an electrical discharge. The radius of the electro sprayed droplet is also a function of the surface tension, liquid density and liquid flow rate V_F :

$$R \propto (V_F^2)^{1/3} \quad (2)$$

Droplets leaving the surface of the cone are charged and accelerated by the electric field towards a counter electrode (Fig. (4)). They lose some liquid due to evaporation which

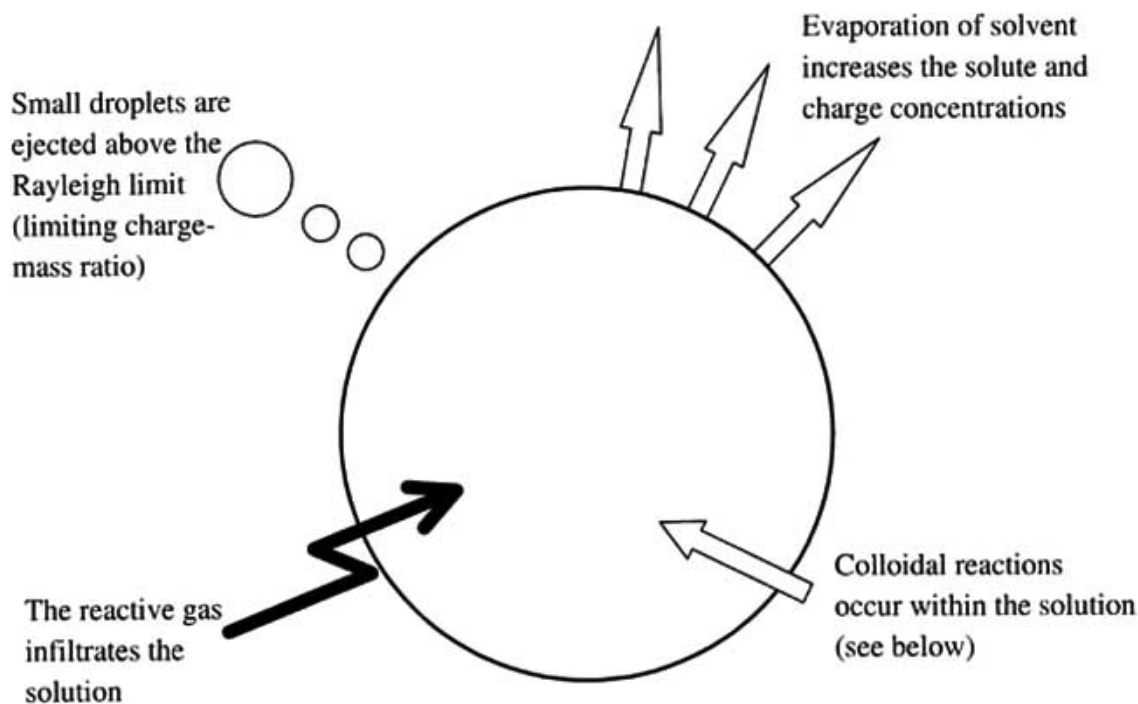


Fig. (4). Fate of emitted droplets.

leads to the growth in surface charge density and consequent Coulombic explosions, which reduce even further the droplet sizes and form satellite droplets containing single ions.

A cone-jet mode depicted in Fig. (3) is just one of the many possible modes. The authors of [29] have tried to classify the known modes in order to reduce confusion and misunderstanding amongst the researchers in electrospray area. They reviewed the modes observed in air and in vacuum and compared them with those in earlier works. They have proposed a terminology to describe non-dripping modes, with the main modes being cone-jet, multi-jet, micro-dripping, simple jet, ramified jet (including fan configuration) and spindle (including harmonic spraying).

Several theoretical models have been developed to describe the processes happening during the electrospray operation. For example in [30] a theory of electrospray transport, evaporation and deposition on a heated substrate was built by studying tracks of single droplets. The authors calculated droplet mass and heat transfer under forced convection and compared them with limiting cases of electrospray transport only or droplet evaporation only. The model also described segregation of primary and satellite electrospray droplets, which is in agreement with experimental data. They conclude that the droplet transport is hardly affected by the diameter of droplet. On the contrary, evaporation can strongly affect the droplet size and salt concentration. Parameters such as substrate temperature, initial droplet diameter and vapor transport may affect the film quality.

The Taylor cone is a very dynamic system, which deforms, oscillates and contains convection flows of charge and mass. It was shown recently [31] that Taylor cone deformations play a central role in the mechanism of electrostatic spraying. In most electrospray regimes spray

currents do oscillate spontaneously. By employing fast time-lapse imaging of the Taylor cone throughout its evolution the authors have demonstrated the presence of a nodal line and standing waves on its surface. They have identified four phases of the cone pulsation cycle (liquid accumulation, cone formation, ejection of a jet, relaxation). Using image analysis they have measured apex velocities, curvatures, and opening angles of the Taylor cone. Singularities in apex velocity during jet ejection were detected. Using light refraction and Fourier analysis, supplemented by electrospray current measurements they established that pulsations in the Taylor cone lead to current oscillations. A stabilization of the spray process can be achieved through monitoring the oscillation frequency and adjusting the spray parameters accordingly.

Progress in electrospray technology would have been impossible without a continuous development of electrospray apparatus. An example of state-of-the art research apparatus that has been developed recently at the Department of Engineering Science, University of Oxford, is shown in Fig. (5).

3. APPLICATIONS OF ELECTROSPRAY IN NANOTECHNOLOGY

3.1 Fabrication of Inorganic Nanoparticles

A great deal of research has been done in the last decade by different groups in an attempt to manufacture and characterise semiconductor quantum dots or nanoparticles with size-dependent physical properties intermediate between those of the bulk solid and molecules [32-37]. This size-dependent variation of physical properties can be explained by a quantum confinement effect. Confinement of electrons and holes within a sufficiently small potential well leads to the disappearance of the continuum of states used to describe a bulk solid. As a result, conduction and valence

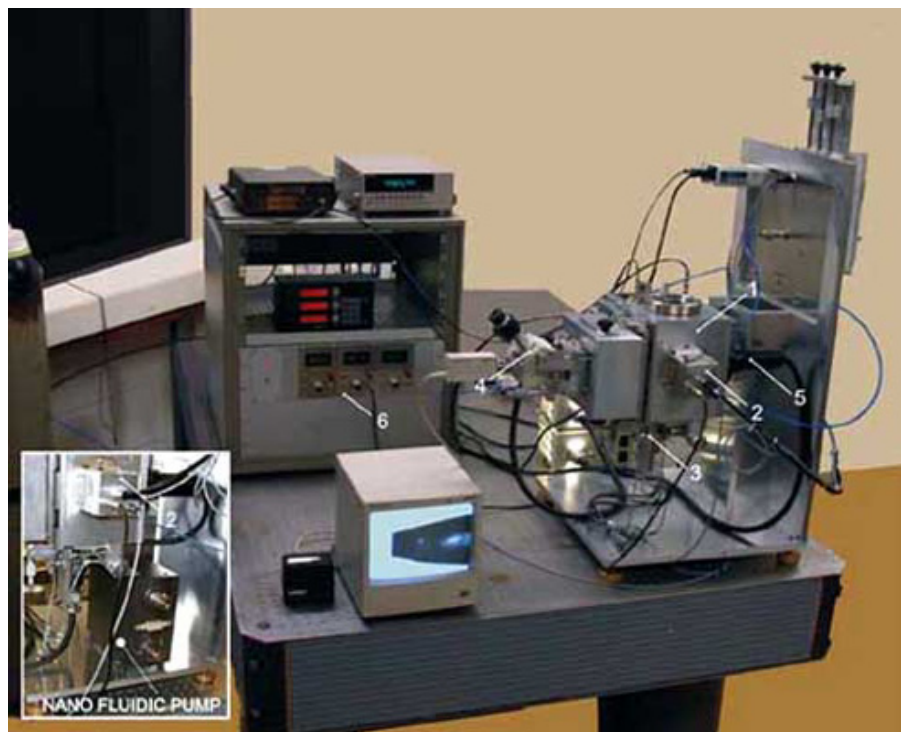


Fig. (5). Electro spray apparatus developed at the Department of Engineering Science, University of Oxford (photo courtesy of Dr Peter Rockett); 1 - sealed test chamber; 2 - electro-spray source assembly; 3 - Faraday collector 3-axis mount; 4 - microscope pan, tilt and focus; 5 - backlighting optics; 6-power supplies and monitoring electronics.

bands are replaced by two sets of discrete energy levels separated by an energy gap, which is approximately inversely proportional to the square of the particle size [38]. This size dependence of energy levels allows one to control properties of nanomaterial that can be applied, for example, to build novel light-emitting devices, electro-optical modulators and lasers [39-41].

In an ideal method of preparation of semiconductor nanoparticles one should be able: 1) to control the average size of the particles; 2) to obtain a very narrow distribution of sizes; 3) to passivate the surface and eliminate surface states; 4) to control the shape of the particles. One of the possible ways to solve these problems simultaneously is to restrict the reaction volume in which the particles are created. This has been done by using various templates like zeolites [42,43], porous glasses [44], micelles [45,46] and polymers [47]. However, these methods are not free from drawbacks.

One of the technologically important group of materials used in semiconductor lasers are III-V materials, especially GaAs. A zero-threshold current operation has been predicted for a semiconductor laser that employs quantum dots as its light generating media. Various techniques have been employed in order to produce GaAs quantum dots, amongst which are electron lithography [48], selective epitaxy [49] and holographic patterning [50], but they usually result in structures with an average size in the 100...500 nm region. Vapour phase nucleation from organo-metallic precursors [51] and non-equilibrium vapour phase synthesis [52] were used to produce GaAs nanoclusters in the range of 10-20 nm and 5-10 nm respectively. However, the GaAs nanoparticles

produced by those methods were quite polydisperse. Colloidal chemistry has been successfully applied to the manufacture of QD of II-VI semiconductors [37] with a narrow size distribution. A similar attempt to produce GaAs clusters resulted in a broad size distribution ranging from 10 to 40 nm [53].

Borrelli et al [54] and Wang and Herron [55] showed that porous glass could be impregnated with GaAs nanoparticles and quantum confinement effects were observed. Justus and co-workers [56, 57] have tried to incorporate GaAs and InP in porous Vycor glass by depositing the III-V onto the porous substrate, followed by heat treatment. However, the distribution of the particle sizes and the average size of the particle in the porous media are limited by the host and are not very uniform.

We have suggested and demonstrated [10-13] that micro-droplets of electrostatically generated aerosol could be used as the restricted reaction volumes for the synthesis of compound semiconductor nanoparticles. We have developed a Gas-Aerosol Reactive Deposition (GARED) technique based on this principle and have applied it to generate some of II-VI and III-V group materials, as well as metal nanoparticles [10-13]. In our technique an aerosol of charged droplets of the spraying solution containing metal ions and polymer molecules is created by an electrostatic field. The aerosol droplets are driven by electrostatic and gravity forces towards the substrate which is held at ground potential.

During the drift of the droplets towards the substrate (Fig. (6)) a reaction takes place between the metal ions inside the droplets and a group VI or V component from the gas phase, and nanoparticles of compound semiconductor

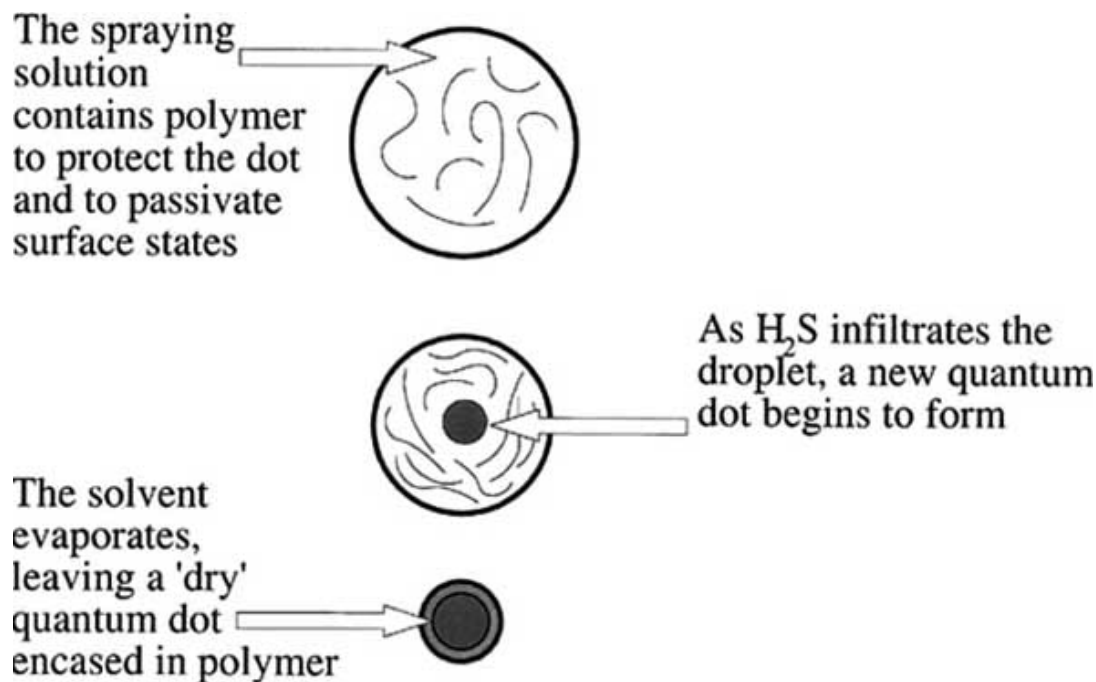


Fig. (6). Process of formation of CdS quantum dot during Gas-Aerosol Reactive Electrostatic Deposition (GARED).

surrounded by a polymer are formed. Finally the solvent is dried out of the droplets and solid particles hit the surface of the substrate. The main point of our technique is that by feeding the aerosol generator with a known concentration of ions and making a known size of aerosol droplet, we can precisely define the number of reactive ions in each droplet and hence the size of the final solid particle.

Our experimental setup is shown in Fig. (2). Polyvinyl alcohol/metal nitrate solution in a water/methanol mixture was supplied from the syringe through the PTFE tubing to the stainless steel capillary which had an inner diameter of 0.2 mm. Aluminium film evaporated onto the top surface of a glass slide or ITO coated glass were used as the substrate which was at ground potential. A variable positive high potential typically of 4-6 kV was applied to the capillary causing a jet of solution to come off the tip of the capillary. Due to the high charge and mutual repulsion of the different parts of the liquid, the jet was broken into uniform micro-droplets and an aerosol was formed under a nitrogen atmosphere. An H_2X gas where X stands for non-metal compound such as S, Se, Te or As, was generated inside the reaction chamber by reacting the appropriate sodium salt with diluted acid. Ions of the metal (Me) in the aerosol droplets react with the H_2X from the gas phase producing MeX nano-particles surrounded by the polymer molecules. The semiconductor /polymer particles were driven by the electric field towards the substrate and deposited onto its surface.

The optical absorption spectra of the nanoparticle films were measured at room temperature with a Philips PU8700 Series UV/Vis spectrophotometer. Several carbon coated copper grids were placed on the top of the substrate in order to obtain TEM samples. A high resolution electron microscope, JEOL4000EX fitted with a top-entry specimen

holder was used to image the single particles and obtain electron diffraction patterns.

Fig. (7) shows room temperature optical absorption spectra of CdS, and GaAs quantum dots. The onset of the absorbance curve for CdS is located at 450 nm and it is shifted towards shorter wavelengths from the bulk value [58] by 70 nm. The slope of the edge of the absorbance curve is steep in accordance with a narrow distribution of particle sizes. The absorption peak which is present at 415 nm (2.98 eV) is due to a 1S-1S quantum dot transition as originally described by Brus [59]. By using the effective mass approximation (EMA) one can estimate that this energy gap corresponds to a spherical CdS quantum dot of 6.2 nm in diameter. The presence of CdS quantum dots was confirmed by a HREM operating at 400 kV. It was observed that on the microscopic scale the polymer film was not deposited evenly, but had thicker areas in the form of submicron semiconductor/polymer agglomerates. Within these thicker areas a high density of nano-crystallites was observed. We suppose these structures to arise from the impact of the micro-droplets on the substrate, and conclude therefore that the solvent had not evaporated completely.

For GaAs quantum dots the onset of the absorbance curve is located at 860 nm and it is blue-shifted from the bulk value [60] by 40 nm. The slope of the edge of the absorbance curve is steep in accordance with a narrow distribution of particle sizes. The particle absorption also shows a tendency to display a weak feature at 795 nm (1.55 eV). We ascribe the peak at 795 nm to the 1s-1s transition [59]. Using the EMA model one can show that this corresponds to an average particle diameter of about 13 nm.

The analysis of the HREM image confirmed the presence of GaAs nanoparticles. The average size of the GaAs nanoparticles determined from the micrographs was 13.4 nm and the polydispersity of the particle sizes was less than

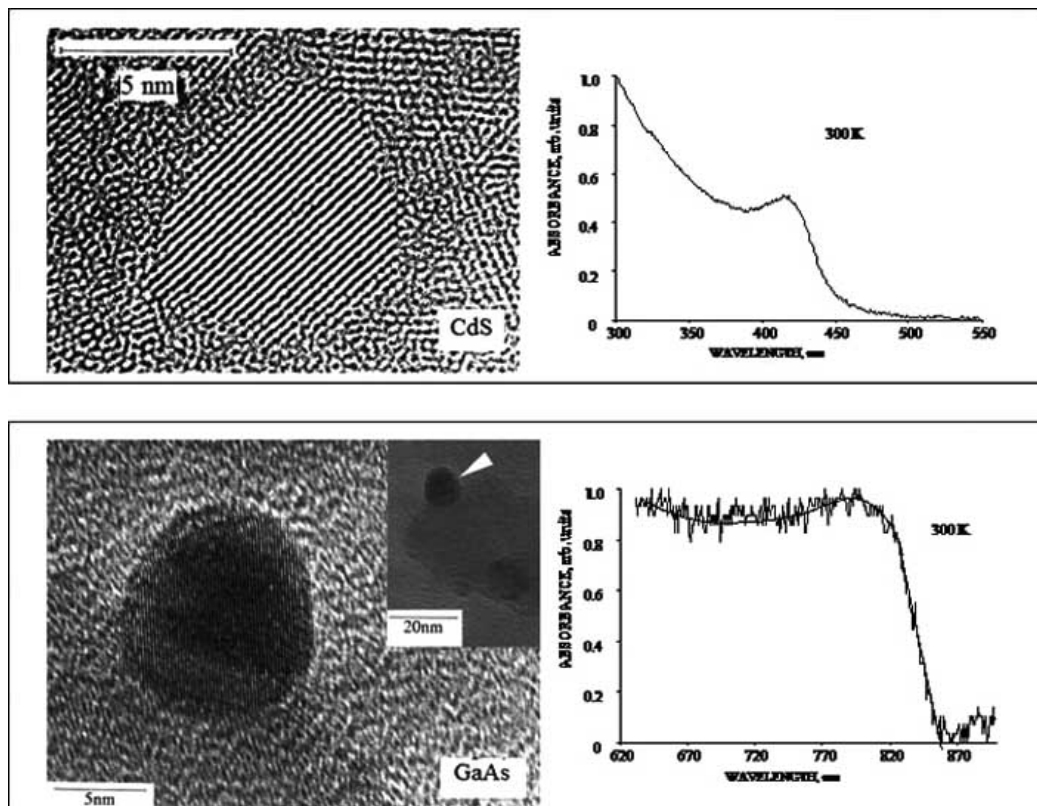


Fig. (7). Optical absorbance spectra and HREM images of GaAs and CdS quantum dots produced by GARED.

10%. The same technique can be applied to generate some metal nanoparticles [13]. A TEM micrograph presented in Fig. (8) shows an array of well separated silver nanoparticles with a HREM image of a single Ag nanoparticle shown as an inset.

The authors of [14] have used electrospray combined with pyrolysis to generate 20 to 40 nm ZnS nanoparticles. A charge neutralising radioactive source has been introduced in order to 1) minimise nanoparticle deposition on the wall of the reactor; 2) reduce the destruction of droplets by Coulombic explosion. A solution containing two components ($\text{Zn}(\text{NO}_3)_2$ and thiourea, $\text{SC}(\text{NH}_2)_2$) that react at 600°C forming ZnS was sprayed into the chamber equipped with radioactive source; generated droplets were neutralised by ions and transported to the pyrolysis furnace. The output of the furnace was fed into the differential mobility analyser (DMA) and condensation nucleus counter (CNC) to be able to measure the sizes and size distributions of the ZnS nanoparticles. TEM was used to confirm the results from DMA-CNC measurements.

Electrospray was performed in a cone-jet mode and a range of concentrations/ conductivities and flow rates were investigated. An agreement in the sizes of produces nanoparticles with a scaling law has been observed. Other electrospray operating modes were also investigated. A concern was raised about the uncertainty in evaporation rates of liquid from the meniscus at the capillary. A use of smaller capillary might alleviate this. Compact and spherical ZnS particles with a standard deviation of 1.3 were produced and efficiently collected thanks to the use of charge-neutralising -source.

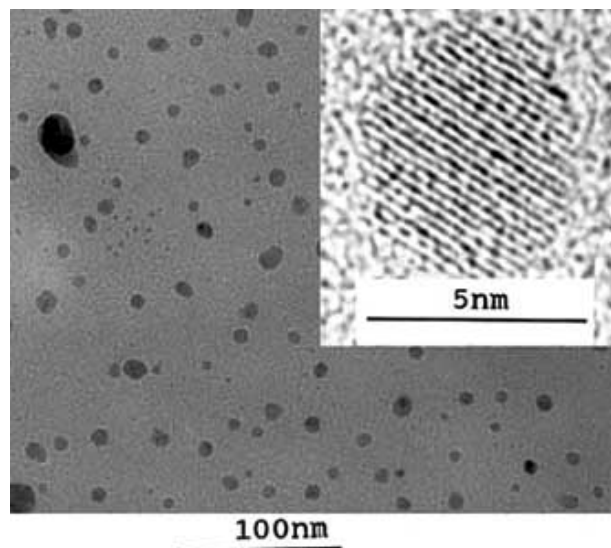


Fig. (8). TEM image of electrosprayed silver nanoparticles; inset shows a HREM image of a single silver nanoparticle.

3.2 Biological and Organic Nanoparticles

The best known biological application of electrospray is that of electrospray ionisation used in mass-spectrometry [8]. The importance of this development was recognised by a Nobel Prize in 2002. Although the technique is used routinely in many labs around the world, the actual physics behind the process of generation of single ions is debated. Another application of electrospray for biological sample

preparation followed in 1992 when the authors of [17] tried to electrospray DNA molecules in order to make samples for a scanning probe microscopy. They observed some breakages and clustering of DNA molecules.

A further very important class of “molecules of life” is proteins. Their size can range between several nanometres to 100 nm and they can be called biological nanoparticles. The number of proteins and their variants that can be expressed by a living cell can be in the region of several tens of thousands. The ability to simultaneously analyse the proteins expressed by a cell could help in better understanding of work of the cellular machinery and, indirectly to solve medical issues. One way to tackle the high throughput analysis of proteins would be by creating a two-dimensional array of different antibodies each capturing a particular protein. Electrospray technique was used by Morozov *et al* to fabricate biologically active protein films [18] and immunochemical micro-arrays of antibodies [58].

In [18] a well studied enzyme, alkaline phosphatase (AP), was sprayed under controlled humidity conditions. The residual activity of the electrosprayed enzyme acted as a measure of functional integrity of sprayed protein. A strong dependence of the residual activity of AP on spraying conditions (voltage and current) was established. The proteins were completely preserved when sprayed in low humidity-low current conditions in the presence of disaccharides acting protectively [18]. In the follow up work [58] a polystyrene membrane filter used as a substrate was replaced with a metallized plastic and spots of antibodies were deposited on its surface through a mask. Low humidity required to preserve the activity of proteins meant that dry protein was deposited on the substrate first and then re-hydrated to allow for covalent bonding to take place. The fabricated arrays worked well for antibody detection using ELISA protocol.

A free standing film of another protein, α -Lactalbumin, was produced by electrospray in [59]. Further cross-linking of the sprayed film resulted in a free standing protein foil. The authors investigated the morphology of the electrosprayed protein films using SEM and SPM. The bioactivity of the electrosprayed protein films was confirmed opening ways to practical exploration of bioactive free standing protein membranes. Other macromolecules that were dispersed or deposited using electrospray include chitosan [60] and it is likely that many more will follow.

3.3 Nano-Coatings and Composites

An interesting application of electrospray to the growth of quantum dot composite media for semiconductor lasers has been developed in [61]. An apparatus that combined an electrospray and organometallic chemical vapour deposition (OMCVD) has been built for that purpose. Quantum dots of CdSe were fabricated by chemical means, size-selected and re-dispersed in a pyridine/acetonitrile mixture. The electrospray has been used to introduce CdSe quantum dots into the growth zone of OMCVD reactor, where it was embedded in the matrix of growing ZnSe, a semiconductor with a band gap that is wider than the band gap of CdSe quantum dots. A glass slide was used as a substrate and a range of deposition temperatures were explored. From the

similarity of the room-temperature absorption and photoluminescence spectra for the initial dispersion and the composite, the authors confirmed a good dispersion of CdSe quantum dots within ZnSe matrix. It has also been confirmed by HREM and SEM. By varying the size of CdSe quantum dots incorporated into the matrix, Danek *et al* have tuned the emission wavelength over a broad spectral region.

Porous ceramic films of ZnO, Al₂O₃ and ZrO₂ as well as mixed compositions were produced in [62] by electrospraying sols derived from metal alkoxide or acetate precursors. The authors chose the cone-jet spraying mode and tried out several designs of the spray nozzles. Higher deposition rates and stability of the cone-jet mode were observed for a large diameter nozzle. Use of a tilted orifice helped to widen both the range of applicable high voltage and the flow rates that produced a stable cone-jet spray. Several designs of the mixing nozzles were tried out. A relatively big deposition area was achieved through the X-Y motion of the substrate. Highly porous ceramic films were produced with morphologies that strongly depend on the substrate temperature. The authors claimed potential applications of electrosprayed nanostructured ceramic films in solar cell production as well as in catalysis.

Apart from organic and biological coatings, electrospray has been used to deposit both polymeric [16] and molecular [63] materials. Deposition of nanostructured polymer films was first demonstrated by Sørensen *et al* in [16] where a cellulose acetate was deposited on top of the glassy carbon electrode in order to create a protective anti-fouling layer. Magnesium perchlorate salt was added to induce film porosity. The electrosprayed film was of better uniformity and offered better protection than a spin-cast film of the same polymer. The porous membrane produced by the electrospray can be used as a size exclusion membrane for voltammetric electrodes.

In a more recent development thin (tens of nanometers) organic films of polymeric materials were obtained by atmospheric-pressure ion deposition based on electrospray technique [63]. The driving force behind this development was a combination of ever-increasing development of electronics, solar cells and light-emitting diodes that are based on organic and polymeric materials and inadequacy of the deposition techniques (PVD, spin-coating and ink-jet printing) used for their fabrication. The authors developed and electrospray apparatus equipped with electrostatic focusing lens and an X-Y stage. The ultimate goal of their development is to be able to sculpture 3-dimensional structures of varied composition out of ionized organic molecules. An additional step of complete drying of the charged droplets was introduced to generate singly or multiply charged ions that were consequently extracted by the electrostatic lens and deposited on the ITO substrate. The resulting films are compact and have an extremely smooth surface. Several polymeric (poly(styrene), poly(methyl-methacrylate)) and biological (angiotensin and insulin) materials were deposited by this technique. Their matrix-assisted laser desorption/ionization time of flight (MALDI-TOF) mass spectra were compared with those of the starting materials and were found essentially identical. In terms of spatial resolution 125 lines per inch were realistic with the

current electrostatic lens but up to 10000 lines per inch can be achieved in theory by using a better lens design. This has been concluded from numerical simulation of the ion flow through the lens with improved design. It was demonstrated that stacks of film containing polymers of similar solubility can be obtained by this technique. This feature could make the proposed technique highly valuable in manufacturing polymer LEDs.

3.4 Nanoparticle and Molecule Characterisation

In our everyday life we are surrounded by an ocean of aerosol particles we breathe and smell. Some of them are produced naturally, like the soot particles from forest fires or the salt particles generated by the sea. Other steadily growing components are by-products of human industrial activity (soot, mineral, metal and radioactive dust) and transportation (fine and ultrafine particles from diesel exhaust). There is also a rapidly increasing category of the engineered or man-made nanoparticles [63, 64]. This growing trend in air pollution by both technogenic and engineered nanoparticles is causing some concerns as this is affecting human health [65-67].

Hence, it is very important to be able to detect and monitor the ultrafine and nano- particles present in the atmosphere. The detection and analysis of submicron aerosol particles can be done in the differential mobility analyser (DMA). In its original form the DMA contains two parallel metal plates with a potential difference applied between them. Introduced charged particles are drifting in the electric field from one plate to another. A steady flow of neutral gas that deflects the particles is blown along the plates. A spatial distribution of the particles on the arriving plate is formed, which reflects particles mass to charge ration. A slit in the receiving plate can be made if particle size selection is required.

For several reasons (Brownian motion, turbulence and space-charge broadening) it is much more difficult to use DMA for analysis of nanoparticles that are below roughly 10 nm in size. The authors of [68] have improved the design of commercial DMA and extended its reliable operation down to 1 nm regime. This was achieved by using electrospray as a source of ions emulating mono-dispersed uniformly charged particles, which were used to calibrate the new DMA design.

A majority of engineered nanoparticles are produced *via* a colloidal chemistry route. Lenggoro *et al.* [69] have developed a simple technique for sizing colloidal particles also using a combined electrospray and DMA/CNC approach. They have performed an on-line determination of size distributions of silica, gold, palladium and polystyrene latex particles with the nominal sizes below 100 nm. Electrospray operating in a cone-jet mode was used to disperse the colloidal suspensions into the aerosol phase. To be useful to DMA the particles were dried and charged to a single positive or negative charge. Electron microscopy and dynamic light scattering were used to verify the results from their apparatus. The size distributions observed by different methods were comparable.

Another work from the same lab [70] dealt with the mineral residues in various types of water. Ultra-pure water

is widely used in semiconductor industry and its quality is critical to the yield of microchips. With the size of transistors rapidly diminishing below 100 nm quality of ultra-pure water is becoming more and more demanding. An electrospray-DMA (ES-DMA) combination was used for that purpose. Interestingly, the ES-DMA technique was capable of detecting residue nanoparticles in the 10-30 nm range that were present even in ultra-pure water.

The progress in sizing nanoparticles stimulated application of ES-DMA technique to biological macromolecules [71]. A charge-neutralised electrospray was combined with a modified DMA and a standard condensation particle counter (CPC). A range of sizes (4-38 nm) corresponding to molecular mass between eight thousand to eight million Dalton was defined by the set up. A very high sensitivity was demonstrated for bovine serum albumin. A broad range of biological macromolecules like DNA fragments and proteins has been characterised using this technique. Pico-mole quantities of sample were sufficient to perform analysis. The equipment is now commercially available from TSI Inc. (Gas-Phase Electrophoretic-Mobility Macromolecule Analyzer- Model 3980).

Finally, in a very recent development, electrospray was used in an ambient mass spectrometry sampling set up [72]. Instead of dissolving substance of interest and then feeding it into the analyzer *via* electrospray, charged droplets of pure solvent were generated and directed to the surface potentially coated with analyte. These droplets ionize and desorb the analyte that leaves the surface to be transferred to the mass-spectrometer. A broad range of analytes have been examined, from simple amino acids through drug molecules, alkaloids, terpenoids, and steroids, to peptides and proteins. The unique feature of this technique is that it works with insulating surfaces. It is likely to find application in forensics and public safety applications. Another fascinating feature of this technique is “*in vivo* sampling of living tissue surfaces”, which allows to detect and monitor the level of medication by sampling person’s skin or saliva.

SUMMARY

Electrospray is one of the most versatile tools available to researchers involved in nanoscience and nanotechnology. It can be realised in a simple apparatus, which nonetheless offers an accurate control of fabrication, dispersion, deposition and analysis of diverse nano-, bio- and molecular materials. A unique capability to generate submicron jets and droplets that can be directed by the electric field makes the electrospray one of the few methods that can be used in direct writing of submicron patterns. It is hoped that this review will further stimulate the utilisation of electrospray across the disciplines.

REFERENCES

- [1] Rayleigh, L. *Phil. Mag.*, **1882**, *14*, 184.
- [2] Zeleny, J. *Physical Review*, **1914**, *3*, 69.
- [3] Taylor, G. I. *Proceedings of the Royal Society A*, **1964**, *280*, 383.
- [4] Cooley, J.F. US Patent 692, 631, **1902**.
- [5] Morton, W.J. US Patent 705,691, **1902**.
- [6] Pugh, E. US Patent 1,855,869, **1932**.

- [7] Dole, M.; Mach, L.L.; Hines, R. L.; Mobley, R.C.; Ferguson, R.C.; Alice, M.B. *J. Chem. Phys.*, **1968**, *49*, 2240.
- [8] Fenn, J. B.; Mann, M.; Meng, C. K.; Wong, S.F.; Whitehouse, C.M. *Science*, **1989**, *246*, 64.
- [9] Fernández de la Mora, J.; Navascués, J.; Fernández, F.; Rosell-Llompart, J. *J. Aerosol Science*, **1990**, *21*, S673.
- [10] Salata, O.V.; Dobson, P.J.; Hull, P.J.; Hutchison, J.L. *Adv. Mater.*, **1994**, *6*, 772.
- [11] Salata, O.V.; Dobson, P.J.; Hull, P.J.; Hutchison, J.L. *TSF*, **1994**, *251*, 1.
- [12] Salata, O.V.; Dobson, P.J.; Hull, P.J.; Hutchison, J.L. *Appl. Phys. Lett.*, **1994**, *65*, 189.
- [13] Hull, P.J.; Hutchison, J.L.; Salata, O.V.; Dobson, P.J. *Adv. Mater.*, **1997**, *9*, 413.
- [14] Lenggoro, I.W.; Okuyama, K.; Fernandez de la Mora, J.; Tohge, N. *J. Aerosol Science*, **1999**, *31*, 121.
- [15] Chen, C.H.; Kelder, E.M.; vanderPut, P.J.; Schoonman, J.M. *J. Mater. Chem.*, **1996**, *6*, 765.
- [16] Hoyer, B.; Sorensen, G.; Jensen, N.; Nielsen, D.B.; Larsen, B. *Anal. Chem.*, **1996**, *68*, 3840.
- [17] Thundat, T.; Warmack, R.J.; Allison, D.P.; Ferrel, T.L. *Ultramicroscopy*, **1992**, *42*, 1083.
- [18] Morozov, V.N.; Morozova, T.Ya. *Anal. Chem.*, **1999**, *71*, 415.
- [19] Lenggoro, W.I.; Xia, B.; Okuyama, K. *Langmuir*, **2002**, *18*, 4584.
- [20] Sobota, J.; Sorensen, G. *Tribology Letters*, **1997**, *3*, 161.
- [21] Nakasoa, K.; Hanb, B.; Ahnc, K.H.; Choib, M.; Okuyama, K. *J. Aerosol Sci.*, **2003**, *34*, 869.
- [22] Signorell, R.; Kunzmann, M.K.; Suhm, M.A. *Chem. Phys. Lett.*, **2000**, *329*, 52.
- [23] Li, D.; Xia, Y.; *Adv. Mat.*, **2004**, *16*, 1151.
- [24] Loscertales, I. G.; Barrero, A.; Guerrero, I.; Cortijo, R.; Marquez, M.; Ganan-calvo, A. M. *Science*, **2002**, *295*, 1695.
- [25] Kruijs, F.E.; Fissan, H. and Peled, A. *J. Aerosol Sci.*, **1998**, *29* 5/6, 511.
- [26] Choy, K. L. in *Handbook of nanostructured materials and nanotechnology*; Nalwa, Ed.; Academic Press, **2000**, 533.
- [27] Duft, D.; Achtzehn, T.; Müller, R.; Huber, B.A.; Leisner, T. *Nature*, **2003**, *421*, 128.
- [28] Yarin, A.L.; Koombhongse, S.; Renekera, D.H. *J. Appl. Phys.*, **2001**, *90*, 4836.
- [29] Cloupeau, M.; Prunet-Foch, B. *J. Aerosol Sci.*, **1994**, *25*, 1021.
- [30] Wilhelm, O.; Mädler, L.; Pratsinis, S.E. *J. Aerosol Sci.*, **2003**, *34*, 815.
- [31] Marginean, I.; Parvin, L.; Heffernan, L.; Vertes, A. *Anal. Chem.*, **2004**, *76*, 4202.
- [32] Henglein, A. *Topics in Current Chemistry*, **1988**, *143*, 113.
- [33] Steigerwald, M.L.; Brus, L.E. *Ann. Rev. Mat. Sci.*, **1989**, *19*, 471.
- [34] Wang, Y.; Herron, N. *J. Phys. Chem.*, **1991**, *95*, 525.
- [35] Fendler, J.N. *Chem. Rev.*, **1987**, *87*, 877.
- [36] Weller, H. *Angewandte Chemie*, **1993**, *32*, 41.
- [37] Efros, A.L.; Efros, A.L.; *Fiz. Tekn. Poluprovodn.*, **1982**, *16*, 1209.
- [38] Arakawa, Y.; Sakaki, H. *Appl. Phys. Lett.*, **1982**, *24*, 195.
- [39] Schmitt-Rink, S.; Miller, D.A.B.; Chemla, D.S. *Phys. Rev. B.*, **1987**, *35*, 8113.
- [40] Vahala, K.J. *IEEE J. Quantum Electron.*, **1988**, *24*, 523.
- [41] Wang, Y.; Herron, N. *J. Phys. Chem.*, **1987**, *91*, 257.
- [42] Wang, Y.; Herron, N. *J. Phys. Chem.*, **1988**, *92*, 4988.
- [43] Kuczynski, J.; Thomas, J.K. *Chem. Phys. Lett.*, **1985**, *89*, 2720.
- [44] Lianos, P.; Thomas, J.K. *Chem. Phys. Lett.*, **1986**, *125*, 299.
- [45] Danhauser, T.; O'Neil, M.; Johansson, K.; Whitten, D.; McLendon, G. *J. Phys. Chem.*, **1986**, *90*, 6074.
- [46] Krishan, M.; White, J.R.; Fox, M.A.; Bard, A.J. *J. Am. Chem. Soc.*, **1983**, *105*, 7002.
- [47] Miyamoto, Y.; Cao, M.; Shingai, Y.; Furuya, K.; Suematsu, Y.; Ravikumar, K.G.; Arai, S. *Jap. J. Appl. Phys.*, **1987**, *26*, L255.
- [48] Nagamune, Y.; Tsukamoto, S.; Nishioka, M.; Arakawa, Y. *J. Cryst. Growth*, **1993**, *126*, 707.
- [49] Ezaki, M.; Kumagai, H.; Toyoda, K.; Obara, M. *Jpn. J. Appl. Phys.*, **1993**, *32*, 1308.
- [50] Sercel, P.C.; Saunders, W.A.; Atwater, H.A.; Vahala, K.J.; Flagan, R.C. *Appl. Phys. Lett.*, **1992**, *61*, 696.
- [51] Sercel, P.C.; Saunders, W.A.; Atwater, H.A.; Vahala, K.J.; Flagan, R.C. *Appl. Phys. Lett.*, **1992**, *60*, 950.
- [52] Uchida, H.; Curtis, C.J.; Kamat, P.V.; Jones, K.M.; Nozik, A.J. *J. Phys. Chem.*, **1992**, *96*, 1156.
- [53] Luong, J.S.; Borrelli, N.F. *Mater. Res. Soc. Symp. Proc.*, **1989**, *144*, 695.
- [54] Wang, Y.; Herron, N. *Res. Chem. Intermed.*, **1991**, *15*, 17.
- [55] Justus, B.L.; Tonucci, R.J.; Berry, A.D. *Appl. Phys. Lett.*, **1992**, *61*, 3151.
- [54] Hendershot, D.G.; Gaskill, D.K.; Justus, B.L.; Fatemi, M.; Berry, A.D. *Appl. Phys. Lett.*, **1993**, *63*, 3324.
- [55] 520 nm
- [56] Brus, L. *IEEE J. Quantum Electron.*, **1986**, *QE-22*, 1909.
- [57] Blakemore, J.S. *J. Appl. Phys.*, **1982**, *53*, R123.
- [58] Avseenko, N.V.; Morozova, T.Ya.; Ataulkhanov, F.I.; Morozov, V.N. *Anal. Chem.*, **2001**, *73*, 6047.
- [59] Uematsu, I.; Matsumoto, H.; Morota, K.; Minagawa, M.; Tanioka, A.; Yamagata, Y.; Inoue, K. *J. Colloid and Interface Sci.*, **2004**, *269*, 336.
- [60] Jayasinghe, S.N.; Edirisinghe, M.J. *J. Mater. Sci. Lett.*, **2003**, *22*, 1443.
- [61] Danek, M.; Jensen, K.F.; Murray, C.B.; Bawendi, M.G. *Appl. Phys. Lett.*, **1994**, *65*, 2795.
- [62] Chen, C.H.; Emond, M.H.J.; Kelder, E.M.; Meester, B.; Schoonman, J. *J. Aerosol Sci.*, **1999**, *30*, 959.
- [63] Saf, R.; Goriup, M.; Steindl, T.; Hamedinger, T.E.; Sandholzer, D.; Hayn, G. *Nature Materials*, **2004**, *3*, 323. (a) Luther, W., Ed. *Industrial application of nanomaterials – chances and risks*, Future Technologies Division of VDI Technologiezentrum GmbH: Düsseldorf, **2004**.
- [64] Salata, O.V. *J. of Nanobiotechnology*, **2004**, *2*, 3.
- [65] Service, R.F. *Science*, **2003**, *300*, 243.
- [66] Englert, N. *Toxicol. Lett.*, **2004**, *149*, 235.
- [67] Ibal-Mulli, A.; Wichmann, H.E.; Kreyling, W.; Peters, A. *J. Aerosol Med.*, **2002**, *15*, 189.
- [68] Rosell-Llompart, J.; Loscertales, I.G.; Bingham, D.; Fernandez de la Mora, J. *J. Aerosol Sci.*, **1996**, *27*, 695.
- [69] Lenggoro, I.W.; Xia, B.; Okuyama, K. *Langmuir*, **2002**, *18*, 4584.
- [70] Han, B.W.; Lenggoro, I.W.; Choi, M.S.; Okuyama, K. *Anal. Sci.*, **2003**, *19*, 843.
- [71] Kaufman, S.L. *J. Aerosol Sci.*, **1998**, *29*, 537.
- [72] Takats, Z.; Wiseman, J.M.; Gologan, B.; Cooks, R.G. *Science*, **2004**, *306*, 15.